EXIT Chart Optimization for a Serial Concatenation of an SCCC and a Space-time Trellis Code

Amit Hooda
Department of Electronics & Computer Engineering, IIT Roorkee
Roorkee, India

Ankur Aggarwal
Department of Electronics & Computer Engineering, IIT Roorkee
Roorkee, India

Alberto Tarable
IEIIT-CNR
Turin, Italy

ABSTRACT

In this paper, we face the design of a space-time trellis code (STTC) to be used in serial concatenation with an SCCC, in order to be iteratively decoded at the coherent receiver. Both Rayleigh and Rice MIMO fading channels are considered. EXIT charts are the key design tool that has been used to optimize the STTC. Simulation results show indeed the advantage of using a recursive STTC w.r.t. using a nonrecursive STTC or even simple spatial multiplexing.

General Terms

Information and communication theory and practice

Keywords

MIMO, Serially Concatenated Convolutional Codes, Space-Time Trellis Codes, Iterative receivers, EXIT charts

1. INTRODUCTION

During the last fifteen years, multi-input multi-output (MIMO) systems have emerged as the key technology solution to satisfy the current need for high-capacity, high-reliability communication links. From a historical perspective, the surge of interest dates back to the works by Foschini and Gans [1] and Telatar [2], which showed that, in the large-SNR regime, the capacity of a $N_t \times N_r$ MIMO channel is equal to $\min(N_t, N_r) \times \log(\text{SNR})$, thus achieving a multiplexing gain with respect to the single-antenna case. Contemporarily, Tarokh et al. [3] proved that the same MIMO channel provides a diversity gain against fading of at most $N_t N_r$. Later, it was realized that these two gains cannot be achieved simultaneously, but that there is a trade-off between them, as shown by Zheng and Tse [4].

Because of the advantages MIMO can offer, a huge array of space-time schemes have been introduced, among which space-time trellis codes (STTCs) [3] are a popular example. A large number of papers also have explored the application of the so-called Turbo principle to MIMO. In Turbo-like space-time receivers, a parallel or a serial concatenation of codes is iteratively decoded like in a Turbo decoder [5]. Often, the inner decoder is simply a MIMO demapper, which accepts feedback from the decoder in order to improve demapping (see [6], [7] and references therein). Gulati and Narayanan [8] propose a serial concatenation of a binary channel code and a recursive space-time trellis encoder. More Turbo-like space-time schemes can be found in [9], [10]. For a comprehensive bibliography on the subject, see also [11].

In this paper, we consider a serial concatenation between an SCCC [12] and an STTC. The novelty of our approach with respect to [8] and similar proposals lies in the fact that we optimize the space-time trellis code through the use of EXIT charts. EXIT charts are a tool introduced by ten Brink **Error! Reference source not found.** to study the convergence of Turbo decoders and similar iterative receivers. In particular, it has been shown that optimality of the iterative decoder (receiver) is achieved when the EXIT charts of the two constituent decoders match. In this paper, for a given SCCC code, we optimize the STTC through trial-and-error search, by finding the best matching between the EXIT chart of the SCCC and the EXIT chart of the STTC. Thus, our paper extends to SCCCs the technique of ten Brink et al. **Error! Reference source not found.**, which have performed the same optimization for LDPC codes.

The structure of the paper is as follows. In Section 2, we describe the channel model and the proposed scheme, devoting Subsection 2.1 to the channel model, Subsection 2.2 to the transmitter and Subsection 2.3 to the receiver. In Section 3, we introduce EXIT charts and we discuss the results of the STTC optimization. In Section 4, we show some simulation results, showing the very good performance in terms of frame error rate (FER) of the optimized STTC as compared to other choices. Finally, in Section 5, we draw some conclusions.

2. CHANNEL MODEL AND PROPOSED SCHEME

2.1 Channel model

We will consider in this paper a fast, flat-fading $N_t \times N_r$ MIMO channel, whose input-output relationship at the i-th time instant is given by:

$$\mathbf{y}[i] = \mathbf{H}[i]\mathbf{x}[i] + \mathbf{n}[i]$$

where $\mathbf{x}[i]$ is the length-N_t transmitted vector, $\mathbf{y}[i]$ is the length-N_r received vector, $\mathbf{H}[i]$ is a N_r x N_t channel matrix of uncorrelated fading coefficients and $\mathbf{n}[i]$ is a vector of zero-mean, uncorrelated circularly-symmetric complex Gaussian rv's with variance $N_0/2$ per real dimension.

Regarding the fading distribution, we will consider two different scenarios:

- a Rayleigh fading model in which all coefficients are zero-mean circularly-symmetric complex Gaussian rv's with variance 1/2 per real dimension;
- a 2x2 dual-polar Rice fading model in which $\mathbf{H}[i]$ is given by a LOS matrix plus a fading term:

$$\mathbf{H}[i] = \beta_1 \begin{bmatrix} \gamma_1 e^{j\varphi_{11}} & \gamma_2 e^{j\varphi_{12}} \\ \gamma_2 e^{j\varphi_{21}} & \gamma_1 e^{j\varphi_{22}} \end{bmatrix} + \beta_2 \mathbf{H}_{Ray}[i]$$

where

$$\beta_1 = \sqrt{\frac{K}{K+1}}, \beta_2 = \sqrt{1-\beta_1^2}$$

$$\gamma_1 = \sqrt{\frac{XPD}{XPD+1}}, \gamma_2 = \sqrt{1-\gamma_1^2}$$

being K the Rice factor, XPD the cross-polar discrimination and $\mathbf{H}_{\text{Ray}}$ a matrix of Rayleigh-distributed fading coefficients (whose variances are equal to the powers of the corresponding elements in the LOS matrix). The phases ϕ_{ij} are chosen independently from a uniform distribution over $[0, 2\pi)$. Such a model is suitable for a 2 × 2 MIMO scheme in which, at each side, the two antennas are orthogonally polarized (e.g., horizontally and vertically), but scattering and antenna misalignment cause some cross-polar power leakage (measured by the cross-polar discrimination).

The channel matrix changes independently of the past at each time instant: such fast fading scenario models, for example, the case in which a large channel interleaver is inserted before transmission. If

$$E\left\{\mathbf{x}^H \mathbf{x}\right\} = E_s$$

then the channel signal-to-noise ratio (SNR) will be given by E_s/N_0.

2.2 Transmitter

The block diagram of the transmitter, equipped with N_t transmitting antennas, is shown in Figure 1.

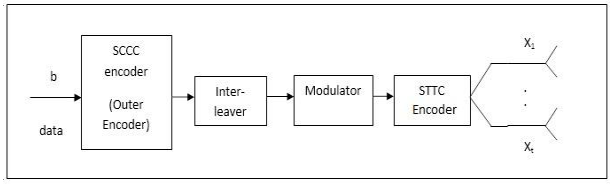

Figure 1: Block diagram of the transmitter

A step-by-step description of the operations performed on the transmitter side is now given.

- The binary information word **b** (of length K_c) is first encded using an SCCC encoder, whose output is a codeword c of length N_c. The code rate is then given by $R_c = K_c/N_c$.
- The codeword **c** is permuted with a random interleaver, obtaining the permuted codeword.
- Codeword is modulated, according to a given modulation format, which will be QPSK throughout this paper. Let us call s the vector of QPSK symbols obtained by modulating.
- The symbol vector **s** is encoded with an STTC encoder, whose output is a space-time codeword matrix **X**, with size $N_t \times L$, where L is the length of the codeword. Each column of **X** is transmitted in parallel by the N_t transmit antennas. The entries of **X** belong to constellation $S = \{\mathbf{s}_0, \mathbf{s}_1, ..., \mathbf{s}_{M-1}\}$ with size $M = 2^m$, which will be QPSK in this paper.

2.3 Receiver

We assume that the receiver has perfect knowledge of the channel coefficients (i.e., we assume a coherent receiver). The block diagram of the receiver is shown in Figure 2.

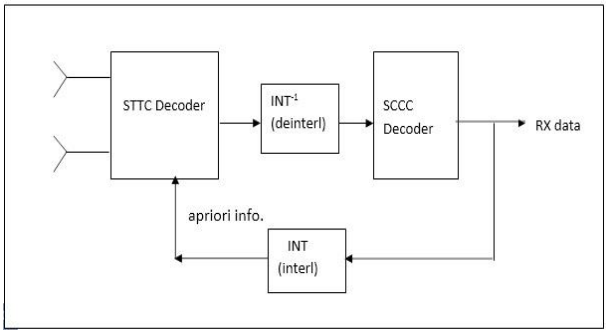

Figure 2: Block diagram of the receiver

The STTC decoder is based on a BCJR algorithm that involves forward and backward recursions **Error! Reference source not found.**. Let us consider the l-th iteration in the decoding process. The STTC decoder has two inputs, the channel output and the feedback from the SCCC decoder, which was computed in the (l - 1)-th iteration. We refer to the latter as the current bit statistics, in the sense that the STTC decoder interprets it as an a priori knowledge on the coded bits of **c**.

For the j-th antenna and i-th symbol interval, M −1 symbol LLRs are computed on the basis of the channel output:

$$LLR_{\text{ch},j}[i,n] = \log \frac{\Pr\{x_j[i] = s_n \mid \mathbf{y}[i]\}}{\Pr\{x_j[i] = s_0 \mid \mathbf{y}[i]\}},\ n = 1,\ldots,M-1$$

In the first iteration, when there is no a priori knowledge on the transmitted symbols, the a priori LLRs are all set to zero. In the hypothesis that such LLRs are uncorrelated (which is almost true because of interleaving), the current bit statistics are used to obtain a priori LLRs on the symbols in **s**. This a priori information, together with the channel LLRs are used to form the branch metrics in the BCJR algorithm.

The output of the STTC decoder (after deinterleaving) is the sequence of updated extrinsic LLRs:

$$LLR_j^{(l)} = \log \frac{\Pr\left\{\mathbf{Y} \mid c_j = 1\right\}}{\Pr\left\{\mathbf{Y} \mid c_j = 0\right\}}, \quad j = 1,\ldots,N_c$$

These are input to the SCCC decoder for another round of decoding, and so on. At the end of the decoding process, the SCCC decoder must also supply estimates of the information bits **b**.

3. EXIT CHART OPTIMIZATION

In this Section, we describe the method used for the optimization of the STTC scheme. Since this method is based on EXIT charts, first we will briefly describe such tool.

3.1 EXIT Charts

EXIT charts, first introduced by ten Brink [13], are useful to study the convergence properties of iterative decoders or receivers. Consider our receiver, which is composed by an STTC decoder and an SCCC decoder exchanging information (in the form of bit LLRs) along a certain number of iterations. In iteration l, we can define the average mutual information between coded bits and the corresponding LLRs fed back to the STTC from the SCCC decoder, which computed them in iteration *l*-1:

$$I_{SCCC\to STTC}^{(l)} = \frac{1}{N_c}\sum_{j=1}^{N_c} I\left(c_j; LLR'^{(l)}_j\right)$$

In the same way, we can define the average mutual information in iteration *l* between coded bits and the LLRs outputs by the STTC decoder, namely:

$$I_{STTC\to SCCC}^{(l)} = \frac{1}{N_c}\sum_{j=1}^{N_c} I\left(c_j; LLR_j^{(l)}\right)$$

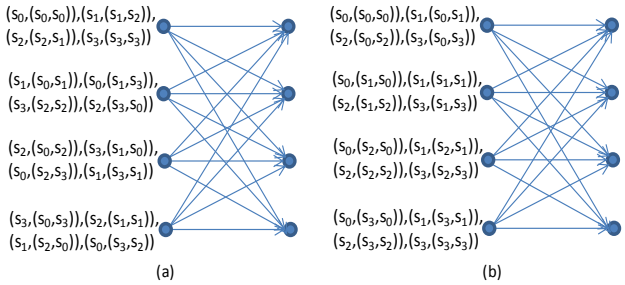

Figure 3: Trellis structure of: (a) the optimized STTC encoder, (b) a nonrecursive STTC decoder

The basic assumption that lies behind EXIT chart theory is that, for sufficiently large interleaver length, the mutual information at the output of a given block is a function of the mutual information at the input. Thus, for the STTC decoder:

$$I_{STTC\to SCCC}^{(l)} = f_{STTC}\left(I_{SCCC\to STTC}^{(l)}\right)$$

and analogously for the SCCC decoder:

$$I_{SCCC\to STTC}^{(l+1)} = f_{SCCC}\left(I_{STTC\to SCCC}^{(l)}\right)$$

where f_{STTC} and f_{SCCC} are the EXIT charts of the two constituent blocks. They can be computed through computer simulations, by breaking the loop in the receiver and injecting bit LLRs obtained from a "fake" AWGN channel to simulate the receiver iterative process. (Notice that the hypothesis of large interleaver length allows neglecting the correlation between the LLR values that are exchanged in the receiver.)

In this way, the evolution of mutual information along receiver iterations can be tracked by placing, as in Figure 4, the two EXIT charts in the same plot, and exchanging the axes for one of the two. Notice that the EXIT chart for the STTC decoder is parameterized by the channel SNR. The point of intersection of the EXIT charts represents the convergence value of mutual information for a sufficiently large number of iterations: if SNR is large enough, this limit point will be close to 1, which means successful decoding. The minimum SNR for which this happens is the convergence threshold of the receiver.

3.2 Optimization Results

In **Error! Reference source not found.**, it is shown that the area between the EXIT charts represents the capacity loss of the system when the two blocks are the constituent blocks of an iterative receiver. It follows that the receiver is optimal when, at the convergence threshold, the two EXIT charts are matched, in the sense that the area between them is minimized.

In view of this principle, we have performed an STTC optimization by searching for the STTC scheme that would best match the SCCC, in the sense of EXIT charts. In particular, we have optimized a 4 states rate-1/2 STTC encoder with one QPSK input symbol and two QPSK output symbols per trellis step. We have resorted to a trial-and-error procedure, since exhaustive research would have required searching among some 350,000 possible mappings, thus being substantially unfeasible.

The optimal scheme we have found has the mapping shown in Figure 3(a). In the figure, the transitions from a given state are labeled from top to bottom, with the input QPSK symbol and the pair of output QPSK symbols. The optimal scheme is a *recursive* STTC scheme, in the sense that two trellis paths that separate at a given time and then merge back some time later correspond to input sequences that differ in at least *two* symbols. This fact is beneficial for the performance of the iterative receiver **Error! Reference source not found.**. On the contrary, for the nonrecursive scheme of Figure 3(b), the two input sequences …$s_0s_0s_0s_0$… and …$s_0s_0s_1s_0s_0$… separate and then merge back, although they only differ in one symbol.

In Figure 4, we show the EXIT charts of the optimized STTC scheme at SNR = 7 dB (blue curve), together with the SCCC decoder one (green curve). As it can be seen, the two curves are well matched. For sake of comparison, we also show the EXIT chart of the nonrecursive scheme of Figure 3(b), at the same SNR (red curve), which is seen not to match the SCCC decoder EXIT curve. Such differences will be confirmed by simulation results, in the next section.

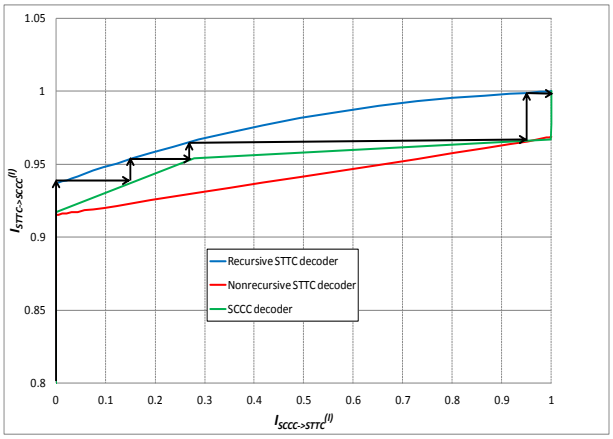

Figure 4: EXIT charts for various schemes (black arrows track the evolution of mutual information along iterations)

4. SIMULATION RESULTS

In this section, we report the simulation results for the proposed STTC scheme, as compared to the following other two choices:

- The nonrecursive STTC scheme whose trellis section is shown in Figure 3(b);
- A simple spatial multiplexing (SM) scheme in which modulated symbols are simply demultiplexed over the two antennas without space-time encoding.

The simulation parameters are as follows:

- QPSK modulation;
- number of transmitting and receiving antennas to 2;
- 15 iterations (max) for the SCCC encoder;
- 10 iterations (max) for the iterative receiver.

We have also simulated the noniterative receiver, where there is no feedback from the SCCC decoder to the STTC. We suppose a genie reveals the SCCC decoder when the information bits are correctly decoded: when this happens, both the SCCC encoder and the receiver (in the iterative case) stop iterating.

We represent the performance of the different schemes in terms of FER as a function of the coded E_b/N_0, which is the signal-to-noise ratio for the coded bits at the output of the SCCC encoder. For the schemes with STTC encoding:

$$\text{coded}\,\frac{E_b}{N_0} = \frac{E_s}{N_0}$$

while for the SM scheme:

$$\text{coded}\,\frac{E_b}{N_0} = \frac{E_s}{2N_0}$$

In Figure 5 we show the simulation results (in terms of FER) for the Rayleigh fading channel. We report the curves for the optimized recursive STTC scheme (blue), the nonrecursive STTC scheme (red) and the SM scheme (green). Solid curves are for the iterative receiver, while dashed curves are for the noniterative one. It can be seen that the optimized STTC scheme with iterative receiver gains about 2 dB (for FER = 1e-3) w.r.t. the nonrecursive STTC scheme and about 1.5 dB w.r.t. the SM scheme. Notice also that the noniterative receiver loses 1 dB against the iterative receiver for the recursive STTC scheme, while the loss is slightly reduced in the other cases.

Figure 6 shows the simulation results for a dual-polar Rice fading channel with Rice factor K = 0 dB and cross-polar discrimination XPD = 20 dB. To distinguish the different curves, we have used the same conventions as for Figure 5. In this scenario, the optimized STTC scheme with iterative receiver gains about 2 dB (for FER = 1e-3) w.r.t. the nonrecursive STTC scheme and as much as about 5 dB w.r.t. the SM scheme. The losses of the noniterative receivers are now reduced w.r.t. Figure 5. To explain the different behavior between STTC and SM in the two scenarios, notice that, while in the Rayleigh case, the maximum diversity gain is 4, in the dual-polar Rice case, it is about 2, because the cross-polar links are quite suppressed: this implies that having a further round of encoding (namely, STTC encoding) is beneficial.

5. CONCLUSIONS

This paper has been devoted to the design of a STTC to be serially concatenated with an SCCC. Using the tool of EXIT charts, we have derived a recursive STTC, whose superior performance on Rayleigh and Rice MIMO fading channels has been demonstrated through simulations.

Future work should investigate ways of reducing the complexity of the receiver (and, possibly, simpler transmitter schemes too) without relevantly compromising performance over a wide range of MIMO channels.

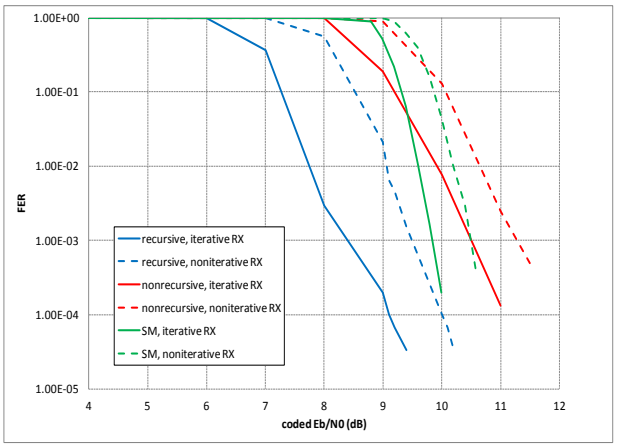

Figure 5: Performance comparison on the Rayleigh fading channel

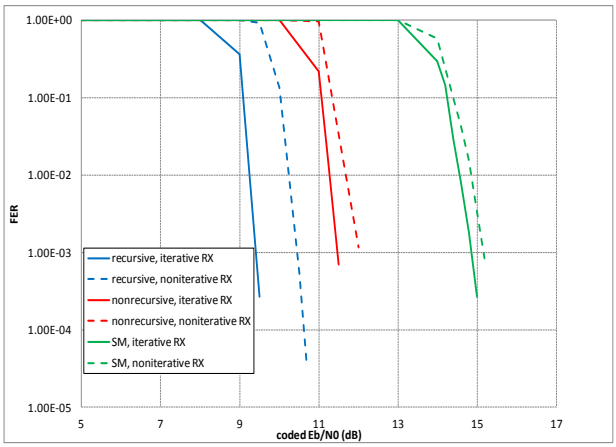

Figure 6: Performance comparison on the dual-polar Rice fading channel (*K* = 0 dB, *XPD* = 20 dB)

6. ACKNOWLEDGMENTS

The authors wish to thank Prof. Guido Montorsi and Prof. Sergio Benedetto for helpful discussions.

7. REFERENCES

[1] G. J. Foschini and M. J. Gans, "On limits of wireless communications in a fading environment when using multiple antennas," Wirel. Pers. Commun., vol. 6, pp. 311-335, 1998.

[2] I. E. Telatar, "Capacity of multi-antenna Gaussian channels," Europ. Trans. on Telecommun., vol. 10, pp. 585-595, Nov./Dec. 1999.

[3] V. Tarokh, N. Seshadri and A. R. Calderbank, "Space-time codes for high data rate wireless communications: Performance criterion and code construction," IEEE Trans. Inform. Theory, vol. 44, pp. 744-765, Mar. 1998.

[4] L. Zheng and D. Tse, "Diversity and multiplexing: a fundamental tradeoff in multiple-antenna channels," IEEE Trans. Inform. Theory, vol. 49, pp. 1073 -- 1096, May 2003.

[5] C. Berrou, A. Glavieux and P. Thitimajshima, "Near Shannon limit error-correcting coding and decoding: Turbo-codes," ," in Proc. IEEE Int. Conf. Commun. (ICC 1993), pp.1064-1070, May 1993.

[6] A. Stefanov and T. M. Duman, "Turbo-coded modulation for systems with transmit and receive antenna diversity over block fading channels: system model, decoding approaches, and practical considerations," IEEE J. Select. Areas Commun., vol. 19, pp. 958-968, May 2001.

[7] A. Tarable, G. Montorsi, and S. Benedetto, "A suboptimum iterative decoder for space-time trellis codes," in Proc. IEEE Int. Conf. Commun. (ICC 2004), pp. 3000-3004, June 2004.

[8] V. Gulati and K. R. Narayanan, "Concatenated codes for fading channels based on recursive space-time trellis codes," IEEE Trans. Wireless Comm., vol. 2, pp. 118-128, Jan. 2003.

[9] Y. Li, B. Vucetic, Q. Zhang and Y. Huang, "Assembled space-time turbo trellis codes," IEEE Trans. on Veh. Technol., vol.54, pp. 1768- 1772, Sept. 2005.

[10] H. Lee, B. Lee, and I. Lee, "Iterative detection and decoding with an improved V-BLAST for MIMO-OFDM systems," IEEE J. Select. Areas Commun., vol. 24, pp. 504 -513, March 2006.

[11] T. Duman and A. Ghrayeb, Coding for MIMO communication systems. Wiley, 2008, Chapter 7.

[12] S. Benedetto, D. Divsalar, G. Montorsi and F. Pollara, "Serial concatenation of interleaved codes: performance analysis, design, and iterative decoding," IEEE Trans. on Inform. Th., vol. 44, pp. 909-926, May 1998.

[13] S. ten Brink, "Convergence behavior of iteratively decoded parallel concatenated codes," IEEE Trans. on Commun., vol.49, pp.1727-1737, Oct 2001.

[14] S. ten Brink, G. Kramer and A. Ashikhmin, "Design of low-density parity-check codes for modulation and detection," IEEE Trans. on Commun. , vol.52, pp. 670-678, April 2004.